AN ANALYSIS ON THE COVERAGE DISTANCE OF LDPC-CODED FREE-SPACE OPTICAL LINKS

Ricardo Luna, Hrishikesh Tapse, Deva K. Borah
Advising Professor: Dr. Deva K. Borah, Associate Professor
Klipsch School of Electrical and Computer Engineering
New Mexico State University
Las Cruces, NM 88003
email: ricaluna, hritapse, dborah @ nmsu.edu
Graduate Category

ABSTRACT

We design irregular Low-Density Parity-Check (LDPC) codes for free-space optical (FSO) channels for different transmitter-receiver link distances and analyze the error performance for different atmospheric conditions. The design considers atmospheric absorption, laser beam divergence, and random intensity fluctuations due to atmospheric turbulence. It is found that, for the same transmit power, a system using the designed codes works over much longer link distances than a system that employs regular LDPC codes. Our analysis is particularly useful for portable optical transceivers and mobile links.

KEYWORDS

LDPC codes, FSO communication, density evolution, log-normal intensity fluctuations.

INTRODUCTION

Free-space optical (FSO) links have many benefits: availability of unlicensed spectrum, availability of large bandwidths, less infrastructure, and more security. However, FSO links are severely affected by atmospheric conditions, such as strong wind, rain or heavy fog. As the light propagates through the atmosphere, a significant portion of light intensity is lost along the propagation path. This is further complicated by atmospheric turbulence that causes random variations in the intensity of the received signal. In order to have reliable links under these conditions, forward error correction (FEC) techniques have been applied to FSO links. However, none of the studies available to date have factored in these parameters in a comprehensive way to analyze the behavior of coded FSO links. In particular, for mobile links or portable devices, it is still unclear how a coded FSO link behaves as the distance between the transmitter and the receiver changes. Note that this is not a simple link budget problem since turbulence characteristics also change with distance.

In this paper, we consider FSO links that use Low Density Parity Check (LDPC) codes as FEC. These codes were first discussed by Gallager in 1962 [1], and were later rediscovered by Sipser *et al.* [2] and MacKay *et al.* [3]. LDPC codes can be divided into two categories: regular and irregular. Regular LDPC codes are such that each node of the same type has the same degree. So, in a (3,6)-regular LDPC code, all the check nodes have a degree of 3 and all the variable nodes have a degree of 6. In the case of irregular LDPC codes, the variable- and check- node degrees are chosen according to some distribution, where, for instance, a third of the variable nodes may have degree 4 and the other two thirds may have degree 6, and similarly for the check nodes. For the same code rate, irregular LDPC codes have been shown to perform better than regular LDPC codes [4].

LDPC codes have been studied extensively for radio frequency (RF) links by many authors, and are shown to achieve close to capacity performance. Richardson and Urbanke proposed a powerful evaluation tool called density evolution [5] that can track the probability of error of an LDPC code for a given noise power level, and can be used to determine the threshold of LDPC codes. By using density evolution, they were able to design an irregular LDPC code that performed just 0.06 dB from capacity [4]. However, density evolution in general is very complicated. A Gaussian approximation of the message densities is used in [6] to simplify density evolution.

Although the behavior of LDPC codes in RF channels is understood well in the literature, the same cannot be said about optical links. FSO links have several unique characteristics that make them very different. In this paper, we consider this problem and make the following contributions. First, we integrate the three major phenomena of optical links, namely, absorption, beam divergence, and turbulence into coded FSO links. Accordingly, we show how to design irregular LDPC codes at various distances from the transmitter. Second, we investigate the behavior of both regular and irregular codes at various transmit distances. Finally, we discuss the relationship between coverage distance of the coded FSO link and atmospheric conditions. We show that by designing appropriate codes, much longer link coverage for the same transmit power can be achieved for FSO links.

SYSTEM DESCRIPTION

We consider intensity modulation with direct detection (IM/DD) using On-Off Keying (OOK). The transmitter is a semiconductor laser of near infrared wavelength. The receiver consists of a combination of a high-gain photodetector, such as an avalanche photodiode (APD), and a transimpedance amplifier. A narrow bandwidth filter is required at the receiver to reduce the effects of undesired ambient light. The received intensity undergoes random fluctuations due to atmospheric turbulence. While most of the work in the literature on coded FSO links considers only atmospheric turbulence, our model here is quite general in that it includes the effects of atmospheric absorption, beam divergence, and intensity fluctuations due to atmospheric turbulence. The effects of these phenomena are described below.

1. *Atmospheric Absorption*: Atmospheric absorption of optical power is modeled by Beer's law as

$$I(\lambda, L) = I(\lambda, 0)e^{-\int_0^L \kappa_\epsilon(\lambda,z)dz} \quad (1)$$

where *I(λ,L)* is the intensity at a propagation distance *L* in km, *λ* is the wavelength, *I(λ,0)* is the initial intensity, and $\int_0^L \kappa_\epsilon(\lambda, z)dz \approx \rho_0 L$, where ρ_0 = 0.1 km^{-1} for clear weather horizontal free-space propagation near the earth's surface [7].

2. *Beam Divergence*: As the beam propagates farther, the received intensity keeps decreasing due to divergence of the beam. The received intensity at a point (*x*,*y*) due to divergence for a Gaussian distributed laser beam propagating in free-space is given by

$$I(x, y, L) = I(\lambda, L)\frac{w_0^2}{w^2(L)} exp\left[-\frac{2(x^2+y^2)}{w^2(L)}\right] \quad (2)$$

where w_0 is the initial beam size (e^{-1} field radius) and *w(L)* is the average beam size (radius) at the receiver [8]. The value of *w(L)* can be found from

$$w(L) = w_0\left[1 + \left(\frac{2L}{kw_0}\right)^2\right]^{1/2}\left[1 + 1.63\sigma_R^{12/5}\Lambda(L)\right]^{1/2} \quad (3)$$

where the wave number, *k*, is $2\pi/\lambda$, σ_R^2 is the Rytov variance for a plane wave, and *Λ(L)* is the Fresnel ratio for vacuum propagation. The Fresnel ratio, *Λ(L)*, is obtained by equations found in the Appendix. The Rytov variance is explained in detail below.

3. *Atmospheric Turbulence*: We consider received intensity at the center of the Gaussian intensity profile of the laser beam. The intensity (irradiance) fluctuation at the receiver is modeled using log-normal distribution [9],

$$f_I(I) = \frac{1}{2I}\frac{1}{(2\pi\sigma_X^2)^{1/2}} exp\left\{-\frac{[\ln(I)-\ln(I(0,0,L))]^2}{8\sigma_X^2}\right\} \quad (4)$$

with

$$E[I] = I(0,0,L)\exp(2\sigma_X^2) \quad (5)$$

where σ_X^2 is the variance of log-amplitude fluctuation of the propagating wavefront, and is related to the scintillation index. The scintillation index, σ_I^2, is the normalized variance of the irradiance fluctuation at the receiver, and is defined as

$$\sigma_I^2 = \frac{\langle I^2\rangle}{\langle I\rangle^2} - 1 \quad (6)$$

where $\langle\cdot\rangle$ is the time average operation. σ_X^2 and σ_I^2 are related by [10]

$$\sigma_I^2 = \exp(4\sigma_X^2) - 1 \quad (7)$$

The strength of atmospheric turbulence can be described by the Rytov variance, σ_R^2, obtained as

$$\sigma_R^2(L) = 1.23 C_n^2 k^{7/6} L^{11/6} \quad (8)$$

where the turbulence structure constant, C_n^2, characterizes the strength of the index of refraction fluctuations [11].

For "weak" turbulence (that is, $\sigma_R^2 < 1$), $\sigma_I^2 \approx \sigma_R^2 \approx 4\sigma_X^2$ [10], [11]. There are two commonly used models for calculating σ_I^2: one for strong turbulence ($\sigma_R^2 > 1$), and one for weak turbulence; both invoke the Rytov variance from (8). For the weak turbulence, it is obtained as

$$\sigma_{I,w}^2 = 3.86\sigma_R^2 \left\{0.4[(1+2\Theta(L))^2 + 4(\Lambda(L))^2]^{5/12} cos\left[\frac{5}{6} tan^{-1}\left(\frac{1+2\Theta(L)}{2\Lambda(L)}\right)\right] - \frac{11}{16}(\Lambda(L))^{5/6}\right\} \quad (9)$$

while for strong turbulence we have,

$$\sigma_{I,s}^2 = exp\left[\frac{0.49\sigma_{I,w}^2}{\left(1+0.56\sigma_{I,w}^{12/5}\right)^{7/6}} + \frac{0.51\sigma_{I,w}^2}{\left(1+0.69\sigma_{I,w}^{12/5}\right)^{5/6}}\right] - 1 \quad (10)$$

where the Fresnel Ratio, $\Lambda(L)$, and curvature parameter, $\Theta(L)$, can be found from equations in the Appendix [8]. The log-amplitude variance, σ_X^2, can then be obtained for the log-normal pdf using (7).

4. *Receiver*: The transmitted laser beam undergoes absorption, divergence, and random intensity fluctuations as described above and arrives at the receiver. The photodetector in the receiver converts the received intensity into a current, which is passed to the transimpedance amplifier to output a measurable voltage. The signal to noise ratio is defined as $T(\eta E[I])^2/2\sigma_n^2$, where η is the responsivity (A m^2/W), T is the bit period, and σ_n^2 is the noise variance. The expectation of the received intensity, $E[I]$, includes the combined effects of atmospheric absorption, beam divergence, and intensity fluctuations. Combining equations (1), (2), and (5) we get

$$E[I] = I_0 \frac{w_0^2}{w^2(L)} \exp\{2\sigma_X^2 - \rho_0 L\} \quad (11)$$

The combined effect of the thermal noise from the transimpedance amplifier and other circuitry along with shot noise from the photodiode is modeled as additive white Gaussian noise (AWGN).

ANALYSIS OF LOW-DENSITY PARITY CHECK CODES

Regular LDPC codes can be characterized by their variable- and check-node degrees, d_v and d_c, respectively. The code rate for regular LDPC codes is given by $r = 1 - d_v/d_c$. Irregular LDPC codes are characterized by their variable- and check-node degree *distribution polynomials*, $\lambda(x)$ and $\rho(x)$, respectively. The coefficients of $\lambda(x)$ and $\rho(x)$ must be nonnegative and $\lambda(1)=\rho(1)=1$. In this case, the maximum degrees for variable and check nodes are often referred to as d_l and d_r, respectively. The code rate for irregular LDPC codes is given by $r = 1 - \int_0^1 \rho(x)dx / \int_0^1 \lambda(x)dx$ [6].

For symmetric RF channels, messages leaving a variable node, v, or a check node, u, are approximated as Gaussian. Let us define the log-likelihood ratio (LLR) for antipodal modulation $u_0 = \log[p(r|x=1)/p(r|x=-1)]$, where u_0 is the LLR message from the channel, x is the bit value of the node, r is the received signal, and $p(r|x)$ is the conditional probability density function (pdf). The message u_0 is Gaussian with mean $2/\sigma_n^2$ and variance $4/\sigma_n^2$, where σ_n^2 is the variance of the channel noise. Since the variance is twice the mean, we need only to track the mean of the message updates for variable and check nodes for each decoding iteration. The variable- and check-node means, $m_v^{(\ell)}$ and $m_u^{(\ell)}$, respectively, are updated as follows [6]

$$m_v^{(\ell)} = m_{u0} + (d_v - 1)m_u^{(\ell-1)} \tag{12}$$

$$m_u^{(\ell)} = \phi^{-1}\left(1 - \left[1 - \phi\left(m_v^{(\ell-1)}\right)\right]^{d_c-1}\right) \tag{13}$$

where ℓ denotes the ℓ-th iteration, and $m_u^{(0)} = 0$ since the initial message from any check node is 0. The work [6] defines $\phi(x)$ as

$$\phi(x) = \begin{cases} 1 - \dfrac{1}{\sqrt{4\pi x}}\displaystyle\int_{\mathbb{R}} \tanh\frac{u}{2} e^{-\frac{(u-x)^2}{4x}} du, & \text{if } x > 0 \\ 1, & \text{if } x = 0 \end{cases} \tag{14}$$

but it is closely approximated by $\phi(x) \sim e^{\alpha x^{\gamma} + \beta}$, for α = -0.4527, β = 0.0218, and γ = 0.86. Equations (12) and (13) can be generalized for irregular codes as [6]

$$m_{v,i}^{(\ell)} = m_{u0} + (i-1)m_u^{(\ell-1)} \tag{15}$$

$$m_u^{(\ell)} = \sum_{j=2}^{d_r} \rho_j \phi^{-1}\left(1 - \left[1 - \sum_{i=2}^{d_l} \lambda_i \phi\left(m_{v,i}^{(\ell-1)}\right)\right]^{j-1}\right) \tag{16}$$

where λ_i and ρ_j are the variable- and check-node degree distribution coefficients respectively [6], and $m_{v,i}^{(\ell)}$ denotes the mean of the message leaving a variable node of degree i. The probability of error is then $P_e = Q\left(\sqrt{m_v^{(\ell)}/2}\right)$, where $m_v^{(\ell)} = \sum_{i=2}^{d_l} \lambda_i \phi\left(m_{v,i}^{(\ell)}\right)$.

Optical channels are asymmetric and, therefore, the above discussion cannot be applied directly. We use an equivalent "symmetricized" channel [12] and write the pdf of the LLR l as

$$\tilde{f}(l) = f(l|\text{on})p(\text{on}) + f(-l|\text{off})p(\text{off}) \tag{17}$$

and error probability $P_e = \int_0^{\infty} \tilde{f}(l)dl$. If we assume equally likely transmitted symbols, (17) reduces to

$$\tilde{f}(l) = \frac{1}{2}\left[f(l \mid \text{on}) + f(-l \mid \text{off})\right] \tag{18}$$

The LLR for the log-normal model is given by

$$L(r) = \ln\left\{\frac{1}{\sqrt{2\pi\sigma_X^2}}\int_0^{\infty} \exp\left[\frac{2rI - I^2}{2\sigma_n^2} - \frac{(\ln(I))^2}{8\sigma_X^2} - \ln(2I)\right] dI\right\} \tag{19}$$

where r is the received electrical signal, and σ_n^2 is the noise variance. The density $f(l)$ is found using a simple transformation of random variables

$$f(l) = f(r)\frac{d}{dr}[L(r)]^{-1} \tag{20}$$

The probability of error obtained using (18) is then mapped to the equivalent probability of error from a Gaussian distribution given as [13]

$$P_e = Q\left(\sqrt{m_{u0}/2}\right) \tag{21}$$

with mean m_{u0} and variance $\sigma^2 = 2m_{u0}$, for $m_{u0} \geq 0$. This mean value m_{u0} is then used as the initial channel LLR mean.

The design of irregular LDPC codes at different distances from the transmitter is carried out using a nonlinear optimization technique called differential evolution as follows [14]:

1. *Channel Characterization*: For a given distance, σ_X is calculated from equations (7) – (10). The equivalent Gaussian initial channel LLR mean, m_{u0}, is then calculated by relating equations (18) and (21), and includes the noise level of the channel.

2. *Initialization*: A cluster of LDPC codes, characterized by $\lambda(x)$ and $\rho(x)$, are generated with the same maximum variable- and check-node degree, d_l and d_r, respectively. Density evolution, given by (15) and (16), is then applied to the cluster of codes with a large number of iterations to determine the probability of error associated with each code for the given noise power level. The code with the smallest error probability is selected.

3. *Mutation*: The selected code is then mutated several times, forming a new "mutated" cluster of codes. This is done to avoid the possibility of a local minimum. Density evolution is applied to this mutated cluster, as it was to the initial cluster, and the code with the smallest probability of error is selected.

4. *Selection*: The probability of error is compared from the best initial cluster code and the best mutated cluster code, and the code with the smallest probability of error is selected.

5. *Termination*: If the probability of error of the selected code converges to a very small value, for example 10^{-7}, the noise power is increased and the process is repeated from Step 1. If the selected code does not perform as desired, the best performing code is mutated and reanalyzed as in Step 3 until either P_e converges to a very small value or a predetermined number of mutations occur.

COVERAGE DISTANCE ANALYSIS AND RESULTS

In this section, we investigate the coverage distance of different LDPC codes. In particular, our aim is to see if a code can be designed for a given transmit power to provide low error rates over a long link distance. Figure 1 shows the minimum required signal to noise ratio (SNR), or threshold SNR, for (3,6) and (4,8) regular codes and irregular codes designed for atmospheric conditions at different distances. As expected, the irregular codes collectively have lower thresholds than the regular codes. Note that the irregular code designed for atmospheric conditions of 2 km consistently performs better than all other codes. We believe that at $C_n^2 = 10^{-15}$, the turbulence statistics at around 2 km provide favorable conditions. The received SNR curve in Figure 1 assumes a constant noise level at all distances. This noise level corresponds to an SNR of 10 dB at a distance of 1 m from the transmitter.

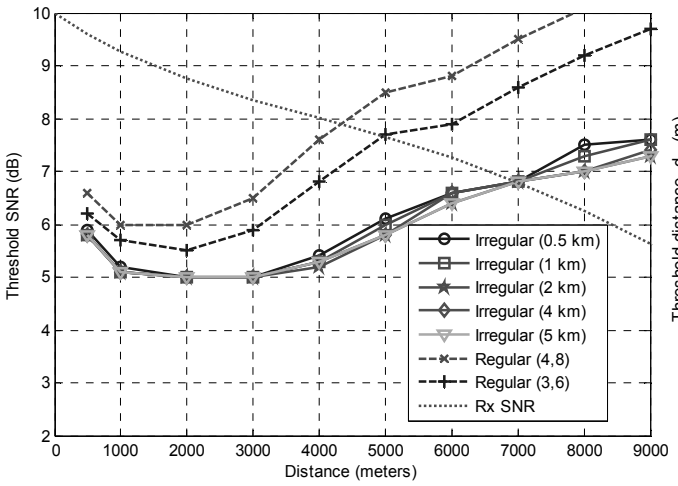

Figure 1. Threshold SNR values at different distances.

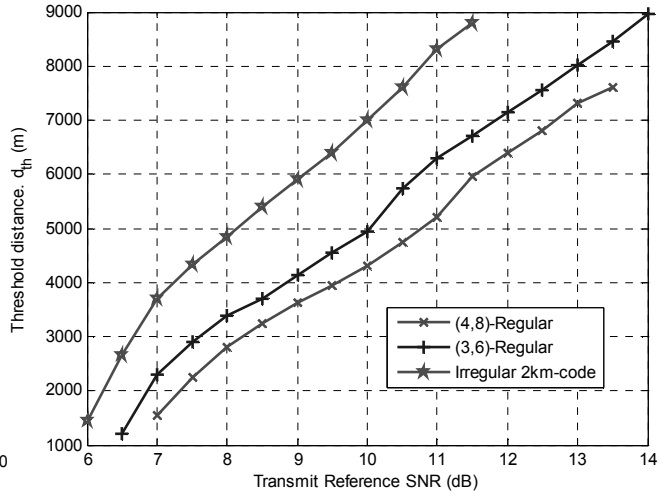

Figure 2. Threshold distance for various codes.

In this paper, we introduce the concept of *threshold distance*, d_{th}. For a given transmit power, it is defined as the distance from the transmitter beyond which the LDPC decoder does not converge. Thus, d_{th} provides an estimate on the coverage distance. In Figure 2, we show d_{th} for various transmit reference SNRs. The transmit reference SNR is defined as the SNR obtained at a distance of 1 m from the transmitter. As expected, d_{th} increases with more transmit SNR. For longer distances, an approximate linear relationship is observed. We model this behavior as $d_{th} = a\gamma_0 + b$, where γ_0 is the SNR at the receiver in dB, and a and b are constants. The constant a is affected by atmospheric channel conditions and b is affected by the particular code. In Figure 3, we show the dependence of a on the extinction coefficient ρ_0 and the turbulence

parameter C_n^2. It is observed that higher ρ_0 and higher C_n^2 lower the value of a. A better code (e.g., designed irregular code) provides a higher value of b.

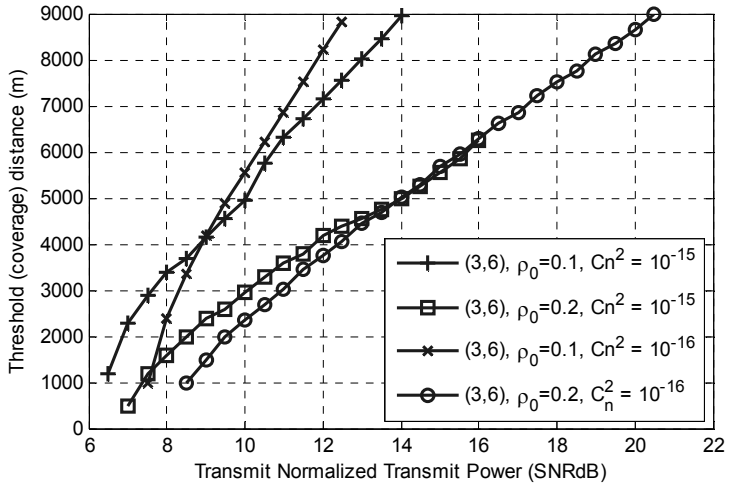

Figure 3. Threshold distance for a (3,6) regular code for different atmospheric channel conditions.

In order to further understand the behavior of LDPC, we plot the additional transmit power required to reach the threshold SNR at various distances in Figure 4. We use the transmit power required for reaching the threshold value at 1000 m as the reference. Observe that at smaller distances the degradation is mainly due to absorption, and turbulence plays a minor role. As the distance increases, both turbulence and absorption become significant.

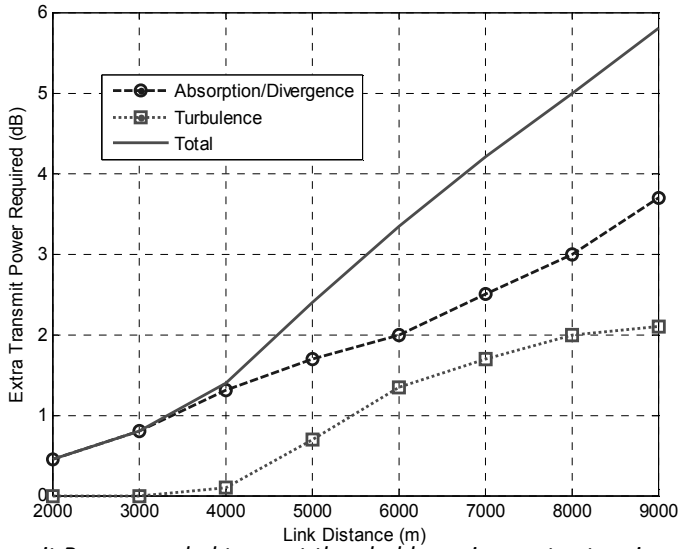

Figure 4. Additional Transmit Power needed to meet threshold requirements at various distances. The reference is 1000 m.

Finally, Figure 5 shows BER values at different distances for the same transmit power. We generate random parity-check matrices, H, to satisfy the variable- and check-node degree distributions for the regular and irregular codes. After 4-length cycles are removed from H, encoding matrices, G, are generated by the greedy algorithm described in [15]. The results are in agreement with Figure 1, showing that the irregular code provides significant improvement in coverage distance over regular codes.

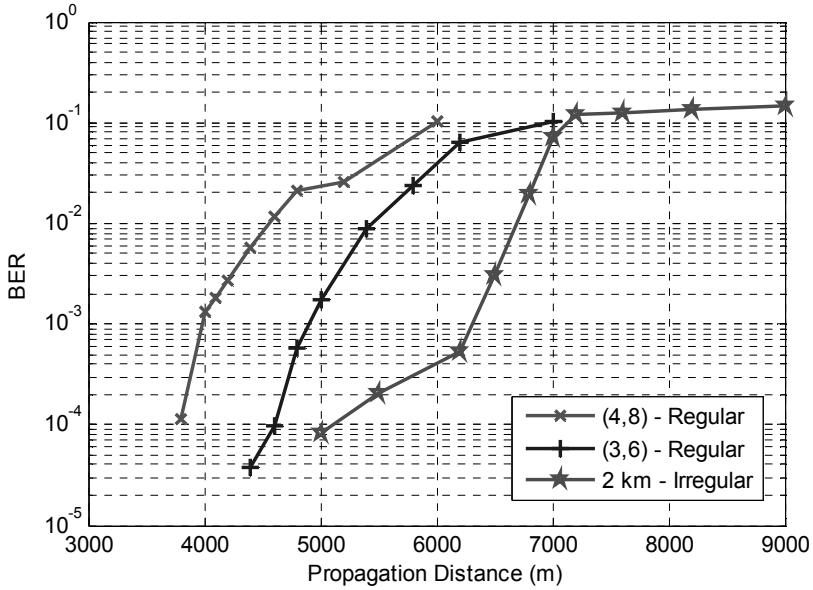

Figure 5. BER for (3,6), (4,8), and designed irregular LDPC code.

CONCLUSIONS

An analysis on the behavior of LDPC codes over various link distances for FSO links is presented. Irregular codes are found to cover a few kilometers longer distances than regular (3,6) and (4,8) codes for the same transmit power.

APPENDIX

The Fresnel ratio, $\Lambda(L)$, and the beam curvature parameter, $\Theta(L)$, are dependent on the initial Fresnel ratio, Λ_0 (L), and curvature parameter, $\Theta_0(L)$ as: $\Theta_0(L) = 1 - L/F_0$, $\Lambda_0(L) = 2L/(k \cdot w_0^2)$, $\Theta(L) = \Theta_0(L)/\left(\Theta_0^2(L) + \Lambda_0^2(L)\right)$, $\Lambda(L) = \Lambda_0(L)/(\Theta_0^2(L) + \Lambda_0^2(L))$, where F_0 is the phase curvature of the beam at the transmitter, and is usually assumed to be infinite for a Gaussian beam so $\Theta_0(L) = 1$ [8].

REFERENCES

[1] R. G. Gallager, "Low-density parity-check codes," *IRE Trans. Inform. Theory*, vol. IT-8, pp. 21–28, Jan. 1962.

[2] M. Sipser and D. A. Spielman, "Expander codes," *IEEE Trans. Inform. Theory*, vol. 42, pp. 1710–1722, Nov. 1996.

[3] D. J. C. MacKay and R. M. Neal, "Near Shannon limit performance of low-density parity-check codes," *Electron. Lett.*, vol. 32, pp. 1645–1646, Aug. 1996.

[4] T. Richardson, A. Shokrollahi, and R. Urbanke, "Design of capacity-approaching low-density parity-check codes," *IEEE Trans. Inform. Theory*, vol. 47, pp. 619–637, Feb. 2001.

[5] T. Richardson and R. Urbanke, "The Capacity of Low-Density Parity Check Codes Under Message -Passing decoding," *IEEE Trans. Inform. Theory*, vol. 47, pp. 599–618, Feb. 2001.

[6] S. Y. Chung, T. Richardson, and R. Urbanke, "Analysis of Sum-Product Decoding of Low-Density Parity-Check Codes Using a Gaussian Approximation," *IEEE Trans. Infrorm. Theory*, vol. 47, pp. 657–670, February 2001.

[7] R. M. Measures, *Laser Remote Sensing: Fundamentals and Applications*. New York, NY: John Wiley & Sons, Inc., 1984.

[8] D. Voelz, X. Xiao, and S.P. Adepu, "Propagation of Narrow Bandwidth Wavelength Radiation Through the Atmosphere," ARL/SLAD, February 2008.

[9] X. Zhu and J. M. Kahn, "Free-Space Optical Communication Through Atmospheric Turbulence Channels Through Atmospheric Turbulence Channels" *IEEE Trans. Commun.*, vol. 50, no. 8, pp. 1293–1300, August 2002.

[10] J. C. Ricklin, S. Bucaille, F.M. Davidson, "Performance Loss Factors for Optical Communication Through Clear Air Turbulence," *SPIE*, vol. 4885, 2002.

[11] L. C. Andrews and R. L. Phillips, *Laser Beam Propagation Through Random Media*. SPIE Optical Engineering Press, 1998.

[12] T. Richardson and R. Urbanke, Eds., *Modern Coding Theory*. Cambridge University Press, 2008.

[13] H. Tapse and D. K. Borah, "Hybrid Optical/RF channels: characterization and performance study using Low-Density Parity-Check codes," submitted to *IEEE Trans. Commun.*, April 2008.

[14] J. Hou, P. H. Siegel, and L. B. Milstein, "Performance Analysis and Code Optimization of Low-Density Parity-Check Codes on Rayleigh Fading Channels," *IEEE J. Select. Areas Commun.*, Issue on *The Turbo Principle: From Theory to Practice I*, vol. 19, no. 5, pp. 924–934, May 2001.

[15] T. Richardson and R. Urbanke, "Efficient Encoding of Low-Density Parity-Check Codes," *IEEE Trans. Infrorm. Theory*, vol. 47, pp. 638–656, February 2001.